Sys Rev Pharm 2021;12(03):809-820
A multifaceted review journal in the field of pharmacy

EGFR Inhibitors and Apoptosis Inducers: Design, Docking, Synthesis, and Anticancer Activity of Novel Tri-Chalcone Derivatives

Menier Al-Anazi [1,2], Melati Khairuddean [1,*], Belal O. Al-Najjar [3,4], Mohammad Murwih Alidmat[1], Nik Nur Syazni Nik Mohamed Kamal[5], Musthahimah Muhamad[5], Maywan Hariono [6]

[1]School of Chemical Sciences, Universiti Sains Malaysia, 11800 Penang, Malaysia
[2]Department of chemistry, Faculty of Science, University of Tabuk, Tabuk 71491, Kingdom of Saudi Arabia
[3]Department of Pharmaceutical Sciences, Faculty of Pharmacy, Al-Ahliyya Amman University, Amman, Jordan
[4]Molecular Modeling and Drug Design Lab, Al-Ahliyya Amman University, Amman, Jordan
[5]Advanced Medical and Dental Institute, Universiti Sains Malaysia, 13200 Kepala Batas,Penang, Malaysia
[6]Faculty of Pharmacy, Sanata Dharma University, Campus III, Yogyakarta, Indonesia

ABSTRACT

Estrogen receptors (ERs) are primarily expressed in cancer cells and interfere with the epidermal growth factor (EGFR) signal pathway. However, data are limited regarding the interaction between cytoplasmic ER expression and EGFR-tyrosine kinase inhibitor response. The objective of this study was to design multi-target molecules for enhancing anti-cancer activity and decreasing drug resistance. Two distinct series of tri-chalcone derivatives **S1(1-7), S2(1-7)** with promising anti-cancer activity was incorporated into the current study. Compounds **S1(1-2)** and **S2(1-2)** demonstrated the highest binding affinity for interactions with the active EGFR binding site. Interestingly, compounds **S1-1** and **S1-2** have shown a potent cytotoxicity of MCF-7 (2.23 ± 0.11 and 2.04 ± 0.71 µM) and MDA-MB-231 (6.44 ± 0.01 and 3.75 ± 0.26 µM), respectively, relative to tamoxifen IC_{50} of 9.3 ± 0.44 and 18.92 ± 1.43 µM. Thus, *in-vitro* EGFR activity was evaluated for compounds **S1-1** and **S1-2**. The results indicated that compounds **S1-1** and **S1-2** showed a significant improvement in the anti-cancer resistant treatment due to their potential effects on the EGFR and the possible anti-ER effect.

Keywords: Tri-chalcones; EGFR inhibitors; AutoDock; anticancer

Correspondence:
Melati Khairuddean
School of Chemical Sciences, Universiti Sains Malaysia, 11800 Penang, Malaysia
Email: melati@usm.my

INTRODUCTION

Today, several cancer treatments available are radiotherapy and surgery for tumors that are localized and systemic treatment such as chemotherapy for cancer that has metastasized due to improved survival and reduced mortality rates (1-4). Chemotherapy is associated with several adverse effects including renal and skin toxicity (1, 2), nausea and vomiting (1, 2, 5, 6). Other effects are drug resistance, leading to treatment failure (4) and reversal of initial reduction of tumor size and cross resistance (7). In breast cancer, combination therapy, immunotherapy, gene therapy, and novel drug delivery are used to overcome resistance but the results are unsatisfactory due to toxicity, and drug-drug interactions (8). These challenges has led to the interest in designing new agents with minimal side effects, less resistance and targeting the tyrosine kinase sub-proteins such as Epidermal Growth Factor Receptors (EGFRs) (8). Strong EGFR expression in breast cancer has been investigated by several studies, in particular the tamoxifen-resistant breast cancer cases (9-11). Hence, targeting the estrogen receptor is not a unique survival track for breast tumors, and the EGFR pathway is an escape way already operating or starting to work. The positive breast tumors of the estrogen receptor (ER-α) that initially possess low or normal levels of EGFR normally gain drastically over-expressed EGFR during the development of the tamoxifen resistance (11, 12). Thus, the combined treatment of the EGFR inhibitor with tamoxifen has demonstrated an improvement in the sensitivity of cancerous cells toward the tamoxifen (13).

EGFR acts as a significant growth signal receptor that regulates cell division and survival (14). As a result, EGFR pathway is currently the target of numerous chemotherapeutic agents (15, 16) including potential small molecule inhibitors such as chalcones (8). The use of small molecule inhibitors is supported by their unique structures which gives them significant affinities and activities against cancer cells (17). Chalcones (aromatic α,β-unsaturated ketones) represent one of the largest classes of plant metabolites such as curcumin and have been reported to have antitumor activities (18-26). In addition, curcumin analogs possess anti-EGFR kinase activity owing to their high hydrogen bonding and hydrophobic interactions (27). In view of this, chalcone molecules are potential anticancer agents that can target the EGFR domain (28). Chalcone has some comparative advantages considering its poor interaction with DNA and low risk of mutagenicity (29, 30). In continuation of our research work on computational docking and molecular dynamics (MD) techniques to examine novel chalcone derivatives as potential EGFR inhibitors and as anticancer agents (31), here we report the synthesis, characterization and *in-vitro* cytotoxicity activity of some tri- and mono-chalcone derivatives against cancerous and non-cancerous breast cell lines. The EGFR kinase inhibitory assay of the compounds was also performed to determine the antiproliferative activity of the multitarget cytotoxic effect.

MATERIALS AND METHODOLOGY

Overview

EGFR tyrosine kinase is a known antineoplastic drug target and novel chalcone derivatives are designed to target this enzyme. The X-ray crystallographic structure of the EGFR kinase domain (PDB ID: 3POZ) with a resolution of 1.5 Å was chosen from Protein Data Bank (PDB); (www.rcsb.org/pdb) (32). AutoDock 4.2 (The Scripps Research Institute, San Diego, CA, USA) was used to study the intermolecular interactions and binding energies of the chalcones within the EGFR active site.

Molecular docking

All chalcone derivatives as shown in Figure 1 were drawn using ACD/ChemSketch; (www.acdlabs.com). Chemical structures were saved in MOL2 format and then converted to PDB files. Ligands PDB files were prepared using AutoDock 1.5.6 Tools; (ccsb.scripps.edu). Once opened, Gasteiger and Kollman charges were added to chalcone derivatives and protein, respectively, and all hydrogen atoms were merged. The three-dimensional grid box was then utilized to select the area of the protein structure to be mapped. The box size was set to 15, 15, and 15 Å. The grid box was centered on the coordinates 16.732, 33.121 and 12.166 (x, y, and z, respectively). Lamarckian Genetic Algorithm (LGA) was used for energy optimization and minimization during docking simulation. Through AutoGrid 4.2, a set of grid maps was created according to the available atom types. Genetics algorithm run was set to 100 while the remaining parameters were kept as default. Molecular docking simulations of new chalcone derivatives and TAK-285 (Control) were performed against 3POZ.PDB using AutoDock 4.2 (33, 34). The conformation with the more negative binding energy was selected as the most suitable conformation. The BIOVIA Discovery Studio Visualizer 16.1 was used to illustrate 2D and 3D docked visualization analysis of the ligands with the amino acids into the EGFR pocket.

Instrumentation and chemicals

FT-IR absorption spectra were obtained by a Perkin Elmer Frontier FT-IR Spectrometer with Perkin Elmer Universal ATR Sampling Accessory (ν, cm^{-1}) in a range of 600 to 4000 cm^{-1}. 1D NMR spectra (^1H, ^{13}C, DEPT-90, and DEPT-135) and 2D NMR (COSY and HSQC) of all compounds were recorded via Bruker UltrashieldTM 500 MHz spectrometer at the School of Chemical Sciences, Universiti Sains Malaysia, Penang, Malaysia. The chemical shifts (δ, ppm) were expressed in (ppm) downfield from tetramethylsilane (TMS) as an internal standard and the coupling constants *(J)* were expressed in Hertz (Hz). Elemental analyses were obtained using Perkin Elmer II, 2400 CHN analyzer. Moreover, the melting point for all the compounds was determined utilizing the Stuart Scientific SMP1 melting point apparatus with an open capillary tube that was used with a temperature range of 25-350 °C. All chemicals and reagents were obtained from Aldrich (Sigma-Aldrich, USA) and were used without further purification.

Synthesis

3.4.1. Synthesis of chalcone based benzene-1,3,5-trichalcone (chalcones **S1-1** and **S1-2**) and nitrilotri (benzene-1,3,5-trichalcone) (chalcones **S2-1** and **S2-2**)

Chalcone (**S1-1** and **S1-2**) and chalcone (**S2-1** and **S2-2**) were synthesized via Claisen-Schmidt condensation reaction (35, 36). In general, chalcone **S1-1** involved the reaction between benzene-1,3,5-tricarbaldehyde (1.5 mmol, 0.250 g) and 1-(4-methoxyphenyl)ethan-1-one (4.6 mmol, 0.694 g) while **S2-1** was formed from the reaction of 4,4',4''-nitrilotribenzaldehyde (1.0 mmol, 0.329 g) and 1-(4-methoxyphenyl) ethan-1-one (3.0 mmol, 0.450 g). Similarly, chalcone **S1-2** involved a reaction between benzene-1,3,5-tricarbaldehyde (1.5 mmol, 0.250 g) and 1-(furan-2-yl)ethan-1-one (4.6 mmol, 0.509 mg) while **S2-2** was formed from 4,4',4''-nitrilotribenzaldehyde (1.0 mmol, 0.329 g) and 1-(furan-2-yl)ethan-1-one (3.0 mmol, 0.330 g). The mixtures were stirred at room temperature in the presence of potassium hydroxide (4.6 mmol, 0.250 g) in 20 mL methanol for 24 hours for **S1-1** and **S1-2**. Reactions for **S1-2** and **S2-2** used potassium hydroxide (3.0 mmol, 0.168 g) in 20 mL ethanol for 72 hours. Thick suspensions of the reactions were formed. Precipitates were filtered off, washed several times with water, and air-dried. Recrystallization from methanol and ethanol gave chalcone **S1-1** (85%) and chalcone **S1-2** (80%) as off-white powders and chalcone **S2-1** (75%) and chalcone **S2-2** (70%) as yellow and red powder, respectively.

Characterization data

(2*E*,2'*E*,2''*E*)-3,3',3''-(Benzene-1,3,5-triyl)tris(1-(4-methoxyphenyl)prop-2-en-1-one), **S1-1**

Yield (85%). White powder. m.p.: 200-202 °C. Molecular weight: 558.63. IR υ_{max}(neat)/cm^{-1}: 3057 (C_{sp2}-H str), 2945, 2830 (C_{sp3}-H str), 1657 (C=O str), 1603, 1589 (C=C str), 1167 (C-O str), 999 - 962 (CH=CH bend *trans*). ^1H NMR (500 MHz, $CDCl_3$), δ_H, ppm: 8.10 (d, *J*=8.5 Hz, 6H, $H^{2''}$); 7.91 (s, 3H, $H^{2'}$); 7.86 (d, *J*=16.0 Hz, 3H, H^{3}); 7.66 (d, *J*=16.0 Hz, 3H, H^{2}); 7.03 (d, *J*=8.5 Hz, 6H, $H^{3''}$); 3.93 (s, 9H, $H^{5''}$). ^{13}C NMR (125 MHz, $CDCl_3$) δ_C, ppm: 55.5 (C-5"), 114.0 (C-3"), 123.6 (C-2), 129.1 (C-2'), 130.7 (C-1"), 130.9 (C-2"), 136.6 (C-1'), 142.2 (C-3), 163.7 (C-4"), 188.2 (C-1). CHN elemental analysis: $C_{36}H_{30}O_6$ Calculated: C, 77.40%; H, 5.41%. Found: C, 77.12%; H, 5.14%.

(2*E*,2'*E*,2''*E*)-3,3',3''-(Benzene-1,3,5-triyl)tris(1-(furan-2-yl)prop-2-en-1-one), **S1-2**

Yield (80%). White powder. m.p.: 220-222 °C. Molecular weight: 438.44. IR υ_{max}(neat)/cm^{-1}: 3115 (C_{sp2}-H str), 1651(C=O str), 1588, 1558 (C=C str), 1160 (C-O str), 999-966 (CH=CH bend *trans*). ^1H NMR (500 MHz,vCDCl$_3$) δ_H, ppm: 7.93 (d, *J*=16.0 Hz, 3H, H^{3}); 7.93 (s, 3H, $H^{2'}$); 7.73 (d, *J*=1.7Hz, 3H, $H^{5''}$); 7.58 (d, *J*=16.0 Hz, 3H, H^{2}); 7.43 (d, *J*=3.6 Hz, 3H, $H^{3''}$); 6.66 (dd, *J*=1.7, 3.6 Hz, 3H, $H^{4''}$). ^{13}C NMR (125 MHz, $CDCl_3$) δ_C, ppm: 112.8 (C-4"), 118.0 (C-3"), 122.9 (C-2), 129.6 (C-2'), 136.3 (C-1'), 142.1 (C-3), 146.8 (C-5"), 153.5 (C-2"), 177.5 (C-1). CHN elemental analysis: $C_{27}H_{18}O_6$ Calculated: C, 73.97%; H, 4.14%. Found: C, 73.79%; H, 3.94%.

(2*E*,2'*E*,2''*E*)-3,3',3''-(nitrilotris(benzene-4,1-diyl))tris(1-(4-methoxyphenyl)prop-2-en-1-one), **S2-1**

Yield (75%). Yellow powder. m.p.: 246-248 °C. Molecular weight: 725.84. IR υ_{max}(neat)/cm^{-1}: 3066 (C_{sp2}-H str), 2926-2836 (C_{sp3}-H str), 1652 (C=O str), 1582, 1567 (C=C str), 1250 (C-N str), 1169 (C-O str), 1101-975 (CH=CH bend *trans*). ^1H NMR (500 MHz, $CDCl_3$) δ_H, ppm: 8.06 (d, *J*=8.5 Hz, 6H, $H^{2''}$); 7.80 (d, *J*=17.0 Hz, 3H, H^{3}); 7.60 (d, *J*=8.25 Hz, 6H, $H^{2'}$); 7.50 (d, *J*=17.0 Hz, 3H, H^{2}); 7.18 (d, *J*=8.25 Hz, 6H, $H^{3'}$); 7.01 (d, *J*=8.5 Hz, 6H, $H^{3''}$); 3.95 (s, 9H, $H^{5''}$). ^{13}C NMR (125 MHz, $CDCl_3$) δ_C, ppm: 55.5 (C-5"), 113.8 (C-3"), 120.6 (C-2), 124.5 (C-3'), 125.6 (C-2"), 129.5 (C-1'), 130.7 (C-2'), 130.8 (C-1"), 142.9 (C-3), 148.1 (C-4'), 163.4 (C-4"), 188.6 (C-1). CHN elemental analysis: $C_{48}H_{39}NO_6$ Calculated: C, 79.43%; H, 5.42%; N, 1.93%. Found: C, 79.23%; H, 5.18%; N, 1.68%.

(2*E*,2'*E*,2''*E*)-3,3',3''-(nitrilotris(benzene-4,1-diyl))tris(1-(furan-2-yl)prop-2-en-1-one), **S2-2**

Yield (70%). Red powder. m.p.: 224-226 °C. Molecular weight: 605.65. IR υ_{max}(neat)/cm^{-1}: 3126 (C_{sp2}-H str), 1653 (C=O str), 1582, 1552 (C=C str), 1322 (C-N str), 1162 (C-O str), 1105-975 (CH=CH bend *trans*). ^1H NMR (500 MHz,$CDCl_3$) δ_H, ppm: 7.87 (d, *J*=17.5 Hz, 3H, H^{3}); 7.67 (d, *J*=1.7 Hz, 3H, $H^{5''}$); 7.62 (d, *J*=8.65 Hz, 6H, $H^{2'}$); 7.41 (d, *J*=17.5 Hz, 3H, H^{2}); 7.35 (d, *J*=3.6 Hz, 3H, $H^{3''}$); 7.18 (d, *J*=8.65 Hz, 6H, $H^{3'}$); 6.62 (dd, *J*=1.7, 3.6 Hz, 3H, $H^{4''}$). ^{13}C NMR (125 MHz, $CDCl_3$) δ_C, ppm: 112.5 (C-4"), 117.3 (C-3"), 120.0 (C-2), 124.4 (C-3'), 130.0 (C-2'), 130.3 (C-1'), 143.0 (C-3), 146.4 (C-4'), 148.4 (C-5"), 153.8 (C-2"), 177.9 (C-1).

CHN elemental analysis: $C_{39}H_{27}NO_6$ Calculated: C, 77.34%; H, 4.49%; N, 2.31%. Found: C, 77.11%; H, 4.19%; N, 2.11%.

In-vitro assays

Cell viability assay

The human breast cancer (MCF7, MDA-MB-231) and non-cancerous breast (MCF-10A) were obtained from the American Type Culture Collection (ATCC, USA). MCF7 and MDA-MB-231 cell lines were cultured in Roswell Park Memorial Institute (RPMI) 1640 and Dulbecco's Modified Eagle Medium (DMEM) media, respectively. MCF10A cell line was cultured in a mixture of DMEM and Ham's F-12 (DMEM/F12) medium. All cell lines were routinely cultured and maintained in a humidified atmosphere with 5% CO_2 at 37 °C. MCF-7 and MDA-MB-231 cancer cell lines were seeded at a density of 1×10^4 cells/well in a 96-well plate. MCF10A was used as control cell lines to determine the selectivity index (SI) values. The cells were treated using fresh assay medium supplemented with an increasing concentration of chalcone derivatives (0-100 µg/mL) within 24-72 hours of incubation at 37 °C. Standard chemotherapeutic drugs including tamoxifen was used as positive controls, while medium alone was used as the negative control (untreated). At each incubation period, 10 µL (5 mg/mL) of 3-(4,5-dimethylthiazol-2-yl)-2,5-diphenyl tetrazolium bromide (MTT) was added into each well, and incubated for 4 hours at 37°C, 5% CO_2. The absorbance of each sample was measured based on the manufacturer's protocol. Half-maximal inhibitory concentration (IC_{50}) values for all cell lines were determined based on Equation 1. The selectivity index (SI) values were calculated as the ratio of the 50% cytotoxic concentration (IC_{50} in cancer cell line) to the 50% cytotoxic concentration on the control cell line (IC_{50} in non-cancerous cell line).

$$\%\text{viable cells} = [(Abs_{sample} - Abs_{blank}) / (Abs_{untreated} - Abs_{blank}) \times 100] \quad \text{..... Equation 1}$$

where, Abs = Absorbance at 570 nm sample (respective compounds or chemotherapeutic drug); blank: Culture medium alone

Recombinant EGFR kinase assay

According to the interactions of compounds **S1-1** and **S1-2** through the molecular docking and dynamics, and their encouraging cytotoxicity findings, these compounds were proceeded to be synthesized. Both compounds were screened for their EGFR inhibitory effect using ADP-Glo™ Kinase Assay (Promega, Madison). The principle of the assay depends on measuring the ADP formed from kinase reaction. Later, this ADP will transform into ATP that generates light and reflects the kinase activity. The assay was conducted according to the company protocol. Positive control contained only 5 µM of ATP-substrate which was used to calculate 100% kinase activity. Negative control (blank) did not contain the inhibitors nor the enzyme and was used to calculate 0% kinase activity. Inhibitors' activities were measured thrice at two distinct concentrations (50 and 0.19 µM). The luminescent signals generated from the ADP-Glo™ assay were converted to percentage activity by subtracting the values of the negative control (0% kinase activity) from all points.

RESULTS AND DISCUSSION

Molecular docking

Molecular docking is used to predict the orientation, type of interaction, and binding energy of ligands within the binding site. In this study, two different series of chalcone compounds (Figure 1) were designed and docked at the active binding site of EGFR and docking scores were compared to TAK 285 (control) as shown in Table 1. The first series of compounds **S1(1-7)** is a tri-chalcone with a benzene ring as the center core system, while the second series of compounds **S2(1-7)** was also a tri-chalcone, but with a nitrogen atom in the central core instead of a benzene ring.

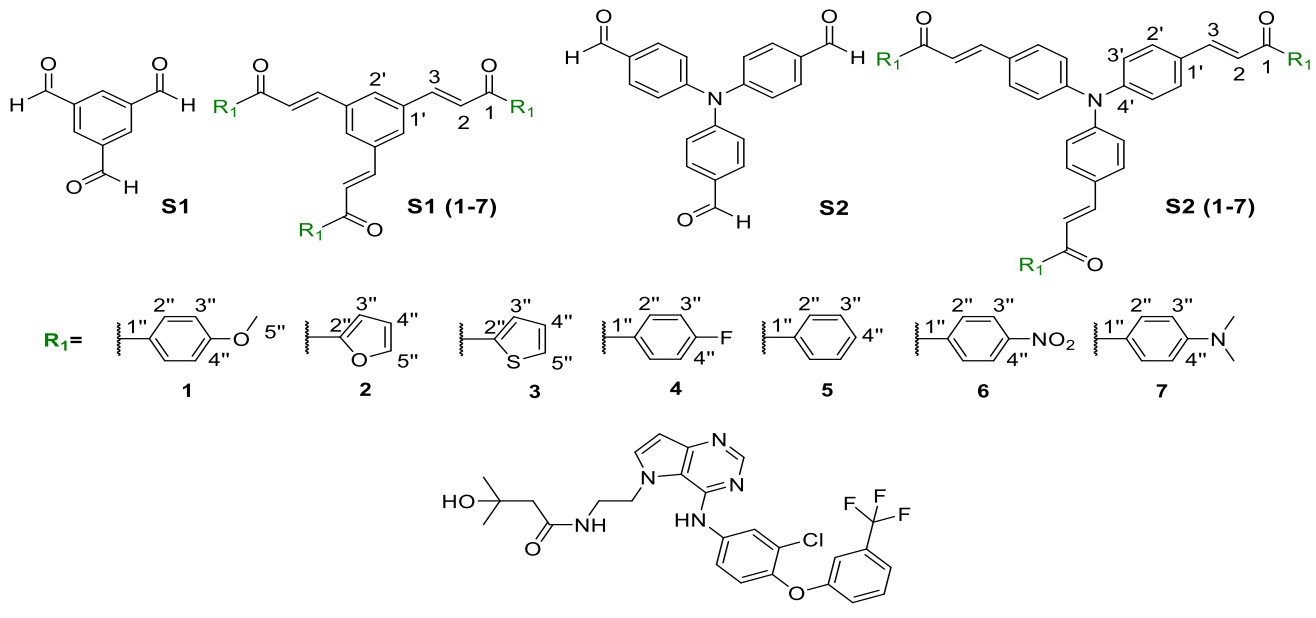

Figure 1: Structures of TAK-285 and novel chalcone derivatives.

A molecular docking study was initiated by control docking of the co-crystallized TAK-285 into the crystal structure of EGFR kinase (PDB ID:3POZ). Control docking showed that TAK-285 reproduced its binding conformation to the EGFR sites with the RMSD of 0.89 Å (Figure 2), and RMSD ≤ 1.0 Å is considered acceptable

(37). Some of the proposed chalcone derivatives had high binding affinities than the control ligand (TAK-285), while others were closer to the control. Moreover, the basic scaffolds of the first series **S1 (**-7.29 kcal/mol) and second series **S2** (-7.44 kcal/mol) displayed less affinity to bind with the active site of EGFR (less negative value than TAK-285 which has a value of -10.15 kcal/mol, as shown in Table 1).

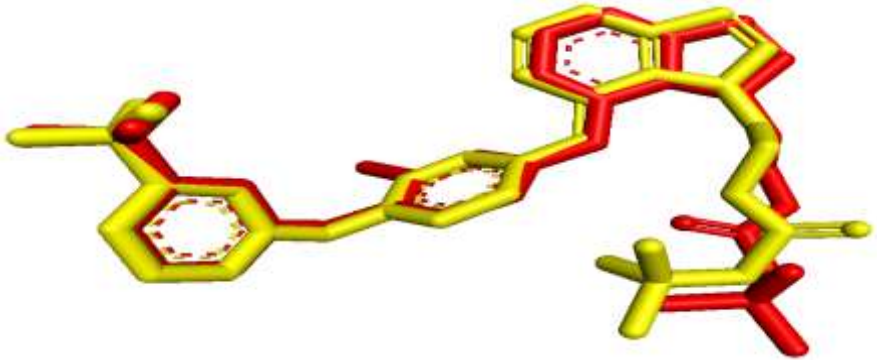

Figure 2: Inset is the superimposition of the TAK-285 crystal structure (red) and docked TAK-285 (yellow) with RMSD = 0.89 Å

Strikingly, chalcone derivatives **S1(1-2)** and **S2(1-2)** showed more negative binding energy and stronger interaction than TAK-285. The formation of a hydrogen bond with the ATP binding site of EGFR (MET 793 and/or LYS 745) might support inhibitory activity (32, 38-40). Table 1 shows the type of amino acids involved in the formation of hydrogen bonds with chalcones derivatives and their free binding energy were used to select prospective chalcones for further analysis and synthesis. The fourteen designs were further pruned down to four compounds (**S1-1**, **S1-2**, **S2-1** and **S2-2**) based on the interaction with EGFR inhibitors (MET 793 and/or LYS 745), and affinity for the binding site with TAK-285. Compounds **S1(1-2)** and **S2(1-2)** bind to the active site, forming several binding interactions with amino acids such as LYS 745, MET 793, ARG 803, THR 854, and ASP 855 as listed in Table 1 and Figure 3. The results were consistent with the findings reported by Subrahmanyam *et al.* (41). Conventional hydrogen bond interactions between the control (TAK-285) and the residues (ARG 776, LEU 777, THR 790, MET 793, ARG 841, and THR 854) were observed within the EGFR pocket. Therefore, compounds **S1(1-2)** and **S2(1-2)** have been selected and synthesized to investigate their cytotoxic activity *in vitro* against several cancer cell lines.

Table 1: Free binding energies (F.B.E) of TAK-285 and the four chalcone derivatives provided by AutoDock 4.2 and the interactive amino acids that formed H-bonds within the EGFR active site.

Compound	F.B.E (kcal/mol)	Interacting amino acids	Compound	F.B.E (kcal/mol)	Interacting amino acids
S1	-7.29	-	**S2**	-7.44	-
S1-1	-12.29	LYS 745, MET 793	**S2-1**	-11.73	LYS 745, ARG 803
S1-2	-12.10	LYS 745, MET 793, THR 854, ASP 855	**S2-2**	-12.09	LYS 745, THR 854
S1-3	-9.14	MET 793	**S2-3**	-9.83	ASP 855
S1-4	-9.73	MET 793, CYS 797	**S2-4**	-9.91	THR 790
S1-5	-9.49	THR 854	**S2-5**	-9.55	ARG 841
S1-6	-9.78	MET 793, ARG 803	**S2-6**	-9.86	MET 793, THR 854
S1-7	-8.18	LYS 745	**S2-7**	-8.97	LYS 745
TAK-285	-10.15	ARG 776, LEU 777, THR 790, MET 793, ARG 841, and THR 854			

S1-1

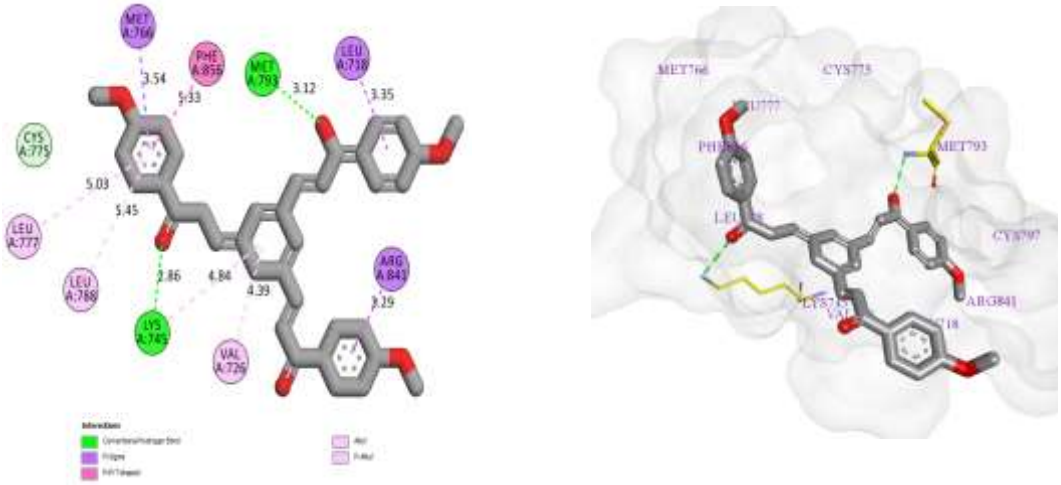
MET A:766
PHE A:856
MET A:793
LEU A:718
CYS A:775
LEU A:777
LEU A:788
LYS A:745
VAL A:726
ARG A:843
MET793
CYS797
ARG841

S1-2

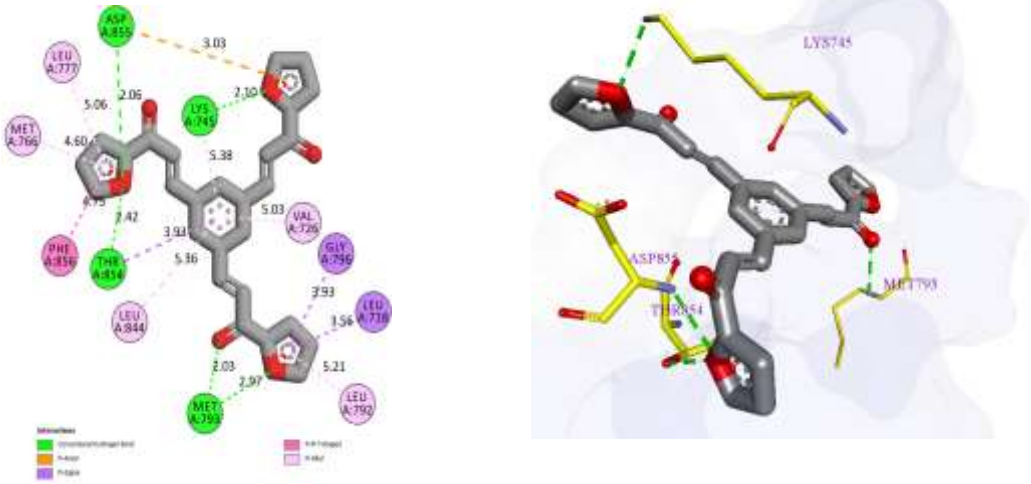
ASP A:855
LEU A:777
MET A:766
LYS A:745
PHE A:856
THR A:854
LEU A:844
VAL A:726
GLY A:796
LEU A:718
MET A:793
LEU A:792
LYS745
ASP855
MET793

S2-1

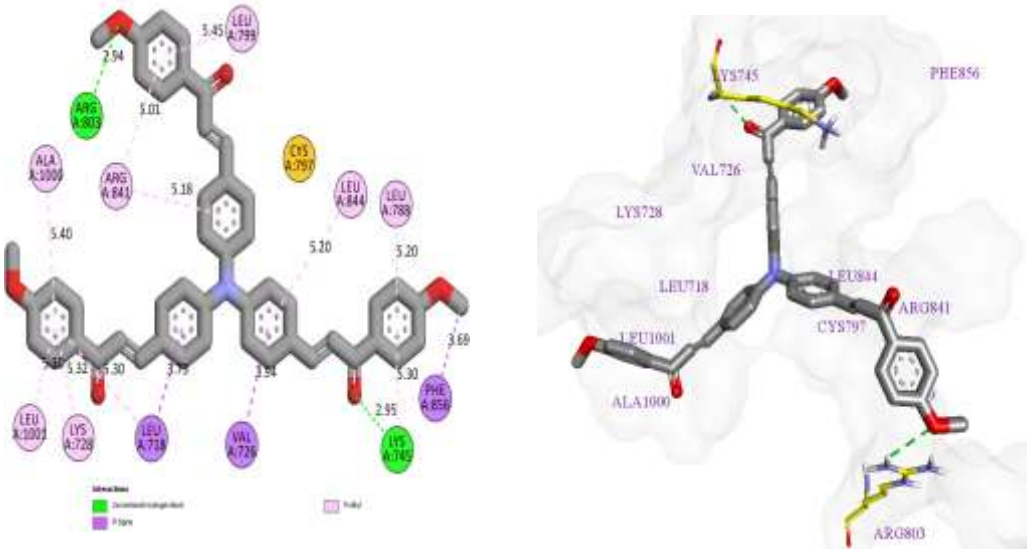
LEU A:793
ARG A:803
ALA A:1000
ARG A:841
CYS A:797
LEU A:844
LEU A:788
LEU A:1001
LYS A:728
LEU A:718
VAL A:726
PHE A:856
LYS A:745
LYS745
PHE856
VAL726
LYS728
LEU718
LEU844
ARG841
CYS797
LEU1001
ALA1000
ARG803

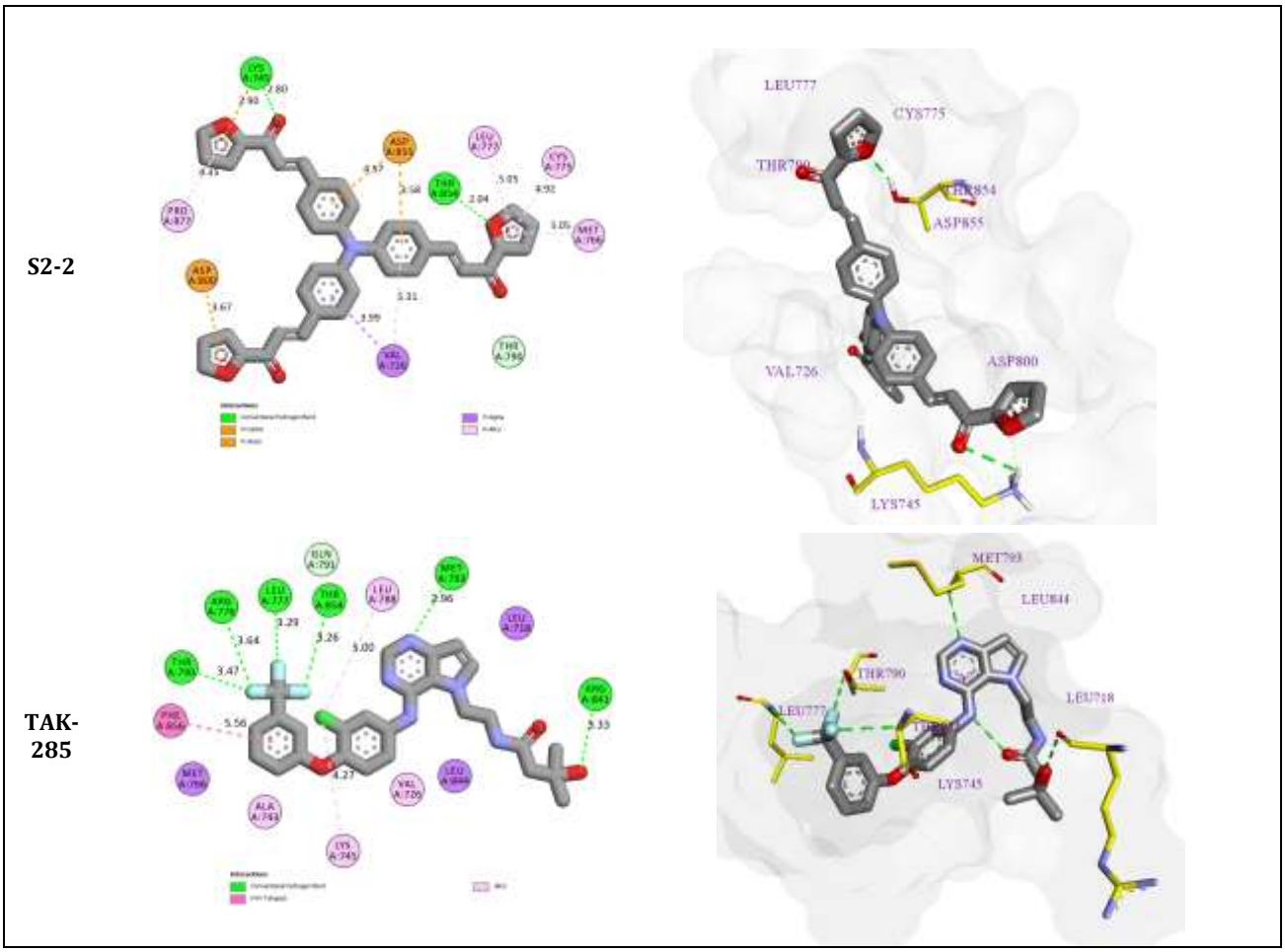

Figure 3: 2D & 3D intermolecular interactions between docked compounds **S1-1**, **S1-2**, **S2-1** and **S2-2** with 3POZ protein. Green and Pink colored amino acids represent their contribution in hydrogen bond and hydrophobic interactions, respectively

Chemistry

The purity of the chalcones was checked by TLC using hexane-ethyl acetate (8:2) solvent system. TLC results showed that only a single spot was observed for each compound. The purified chalcones have melting points measured by open capillary tubes. The structures of all these chalcones were confirmed by FT-IR, ^{1}H-NMR, ^{13}C-NMR and CHN elemental analysis.

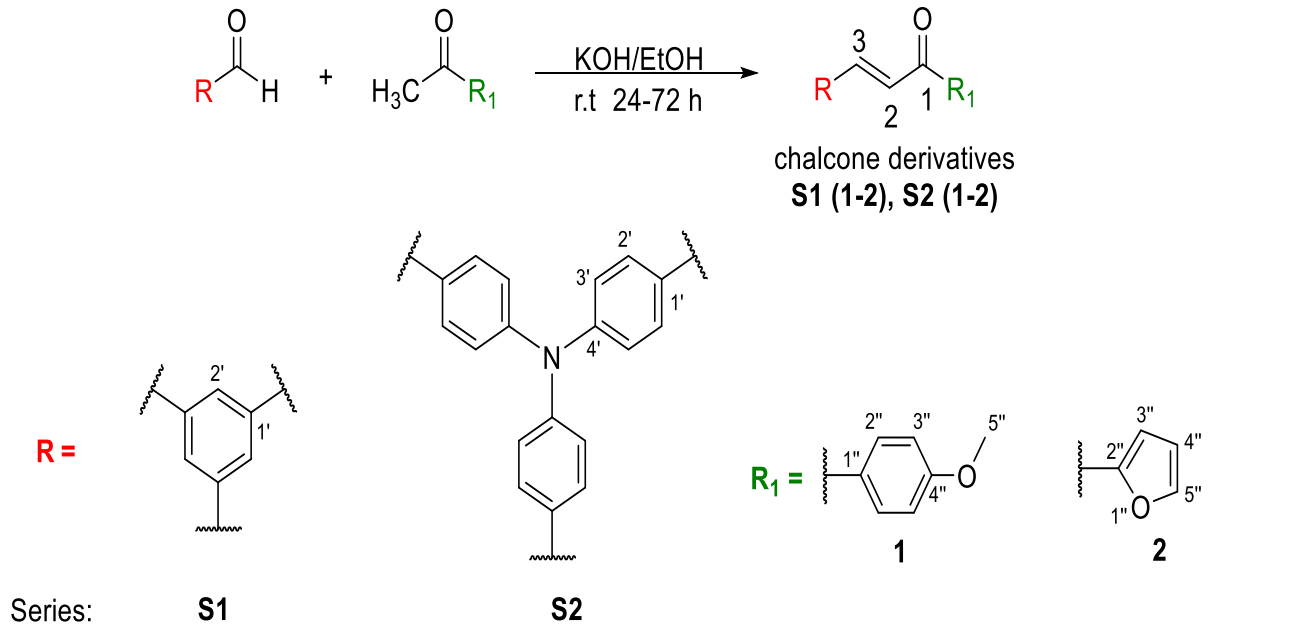

Scheme 1: Synthesis pathway of chalcone derivatives.

From the molecular docking data of tri-chalcone **S1(1-7)** and **S2(1-7)**, only compounds **S1(1-2)** and **S2(1-2)** were selected to be further investigated. The IR spectra of these compounds showed a characteristic absorption band at υ 3057-3126 cm^{-1} (C_{sp^2}-H str) while in chalcones **S1-1** and **S2-1**, the absorption bands were observed at υ 2945-2830 cm^{-1} (C_{sp^3}-H str). The spectra also recorded two intense absorption bands at υ 1657-1651 cm^{-1} and 1603-1582, 1589-1552 cm^{-1} that were related to the carbonyl (C=O) and alkene (C=C) of the chalcone and the aromatic ring (C=C), respectively. Also, the absorption bands at υ 1105-962 cm^{-1} were attributed to CH=CH bending (*trans*).

The ^{1}H NMR spectra (in $CDCl_3$) of these chalcones showed two doublets at δ_H 7.41-7.93 with a coupling constant of 16.0–17.5 Hz that confirmed the generation of chalcones with an α,β-unsaturated ketone. This higher coupling constant value indicates that both compounds were successfully isolated as an *E*-isomer. A singlet at δ_H 7.90 corresponds to the aromatic proton ($H^{2'}$) in the center of the benzene ring which has three isolated protons in both chalcones **S1-1** and **S1-2**. Two doublets at δ_H 7.18 and 7.6 were assigned to $H^{3'}$ and $H^{2'}$ for the symmetrical three benzene rings with two types of aromatic protons in both chalcones **S2-1** and **S2-2**. Compounds **S1-2** and **S2-2** (furan ring) showed a doublet at δ_H 7.73-7.67 and δ_H 7.43-7.35, corresponding to $H^{5''}$ and $H^{3''}$ protons, respectively, while $H^{4''}$ proton showed a triplet at δ_H 6.66-6.62. Compounds **S1-1** and **S2-1,** displayed the aromatic signals as two doublets at δ_H 8.10-8.06 and δ_H 7.03-7.01 for $H^{2''}$ and $H^{3''}$, respectively. Compounds **S1-1** and **S2-1** showed a singlet at δ_H 3.95-3.93 due to $H^{5''}$ proton for the methoxy group as shown in Figure 4.

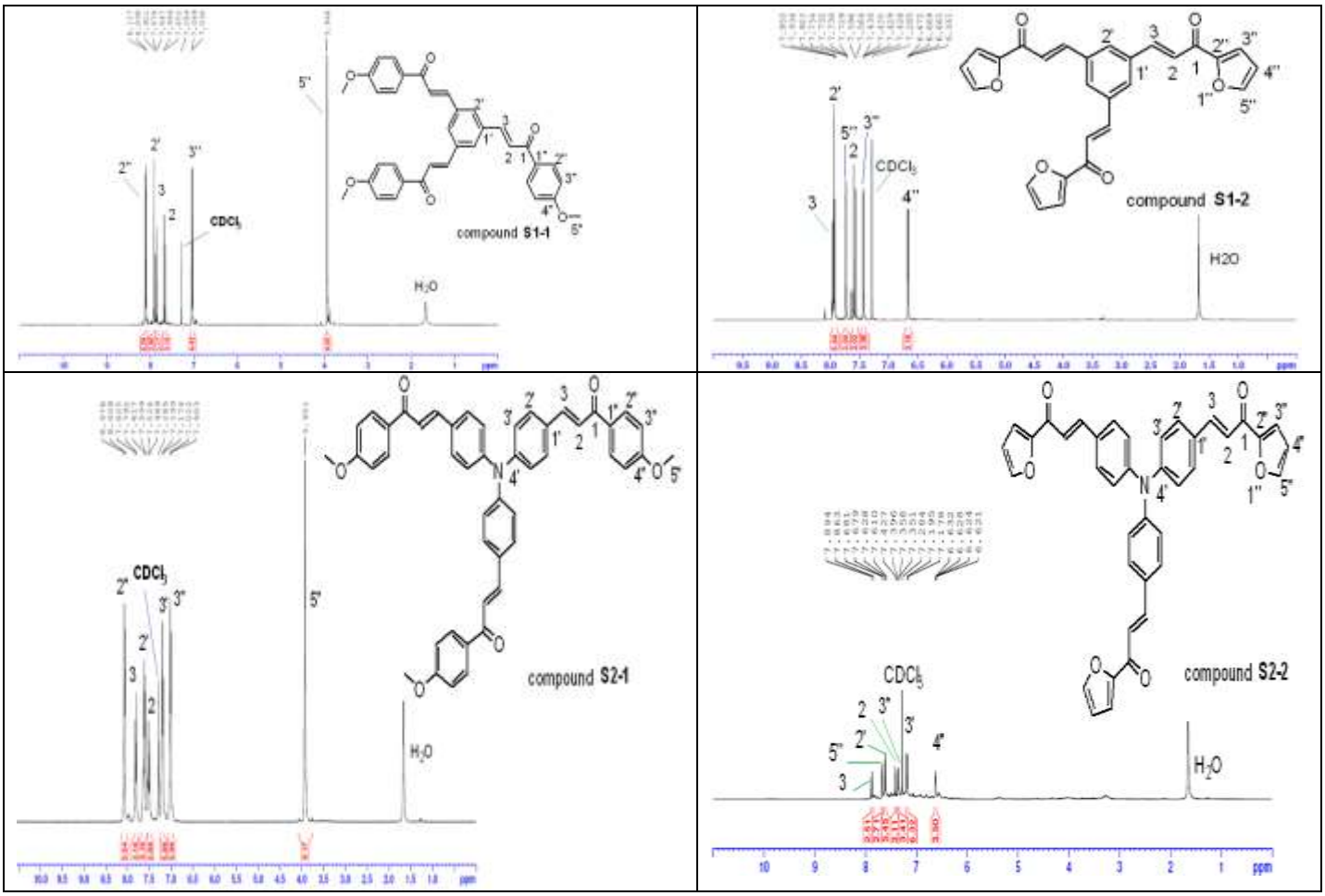

Figure 4: ^{1}H NMR spectra of chalcones **S1(1-2)** and **S2(1-2)** in $CDCl_3$

The ^{13}C-NMR spectra of all the chalcone derivatives showed the common signals which were recorded at δ_C 188.6-177.5 for the carbonyl carbon, δ_C 123.6-120.0 and δ_C 142.1-143 for the alkene group, **C**H=**C**H and δ_C 163.7-112.5 for all the aromatic carbons. For chalcones **S1-1** and **S2-1**, the signal for the methoxy carbon (O**C**H_3) was observed at δ_C 55.5, as shown in Figure 5c. The spectra of DEPT-90 and DEPT-135 NMR confirmed all the methine (CH), methyl (CH_3) and quaternary carbons (C) in compound **S1-1**, as shown in Figure 5(d,e). The extreme upfield signals at δ_C 55.5 was assigned to the methoxy carbon at $C^{5''}$. The quaternary carbons ($C^{1'}$, $C^{1''}$, $C^{4''}$) in chalcone **S1-1** were identified through their absence in the DEPT-90 and DEPT-135 spectra.

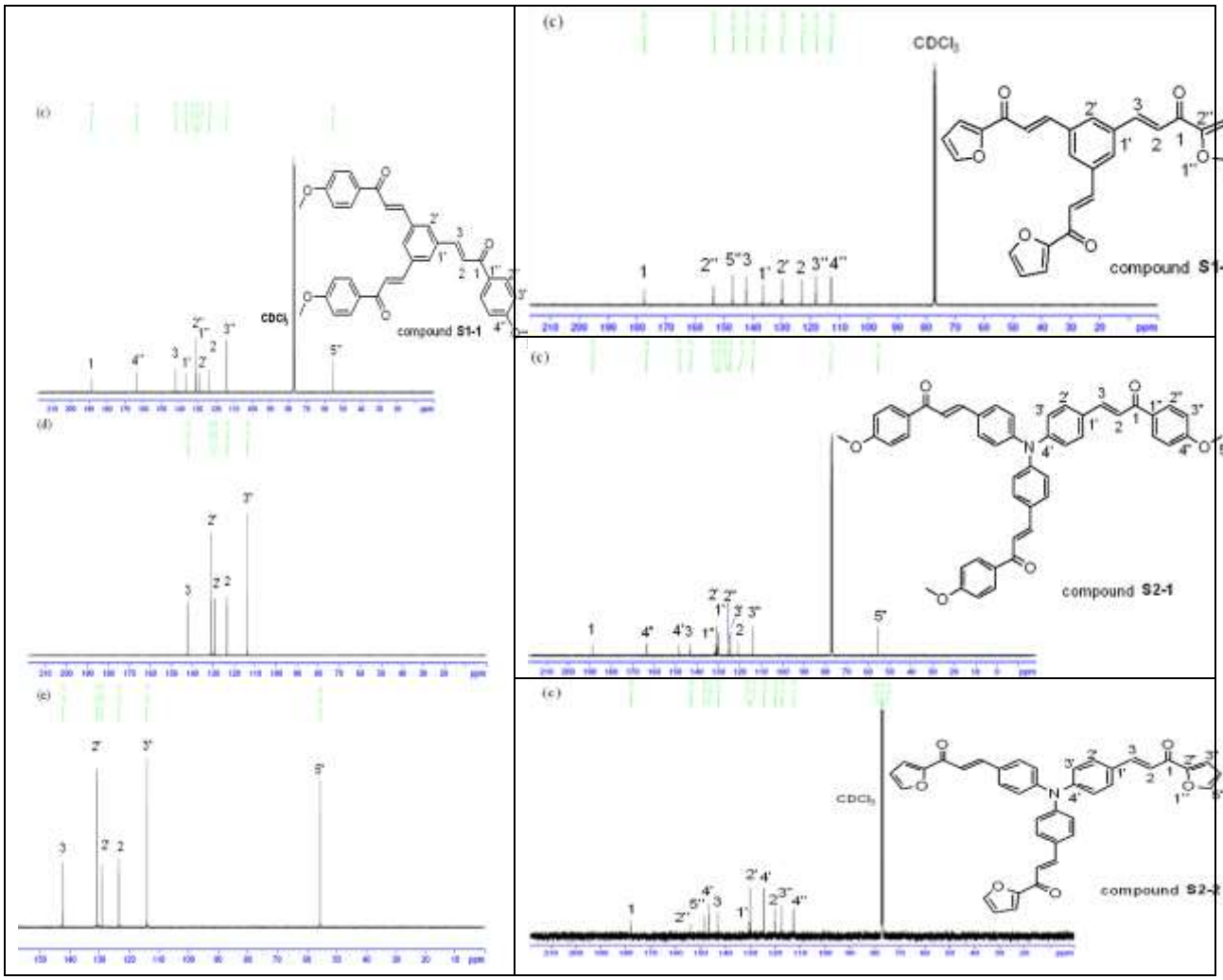

Figure 5: (C) ^{13}C NMR, (d) DEPT 90 and (e) DEPT135 spectra of chalcones **S1(1-2)** and **S2(1-2)** in $CDCl_3$.

The 2D-NMR correlation using ^{1}H-^{1}H COSY and ^{1}H-^{13}C HSQC (Figure 6) spectra were used for unambiguous assignment. ^{1}H-^{1}H COSY spectra of chalcone **S1-1** showed the correlation of $H^{3''}$ with $H^{2''}$, H^{2} with H^{3}, H^{3} with H^{2}, $H^{2''}$ with $H^{3''}$. On the other hand, the ^{1}H-^{13}C HSQC spectrum revealed the correlations between the proton and carbon. A cross peak was observed between the methoxy proton $H^{5''}$ at δ_H 3.93 with the methoxy carbon $C^{5''}$ at δ_C 55.5. A cross peak was also observed between H^{2} and H^{3} protons at δ_H 7.66 and δ_H 7.86 with the methine carbons C^{2} and C^{3} resonated at δ_C 123.6 and δ_C 142.2, respectively. Finally, The remaining three aromatic protons, $H^{3''}$, $H^{2'}$ and $H^{2''}$ in chalcone **S1-1** which appeared at δ_H 7.03, 7.91 and 8.10 gave a cross peak with methine carbon at δ_C 114.0, 129.1 and 130.9, respectively. All the carbons were determined and figuratively represented in Figure 5.

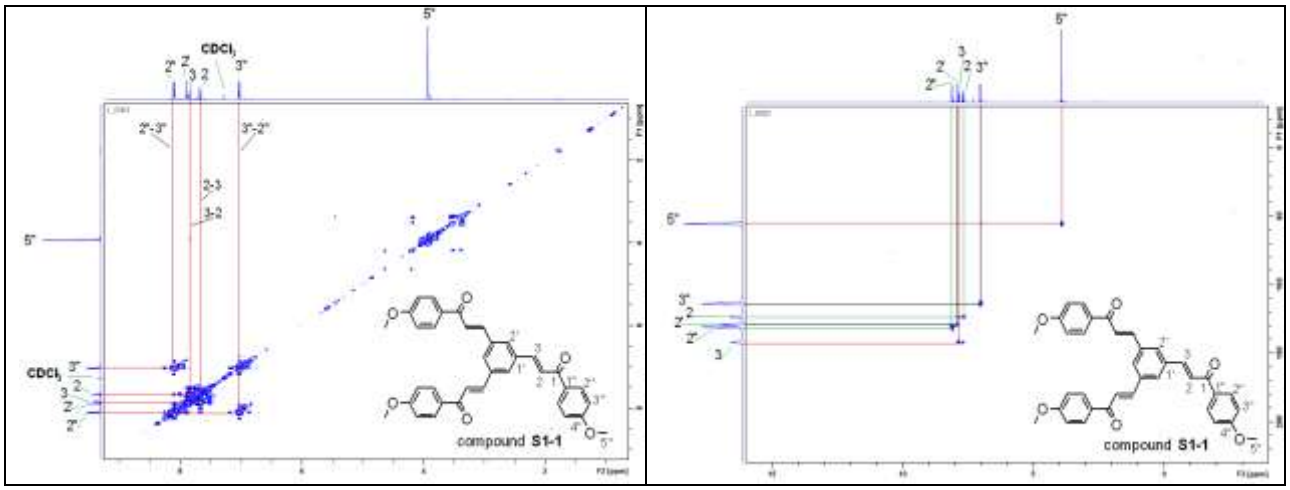

Figure 6: ^{1}H-^{1}H COSY, ^{1}H-^{13}C HSQC NMR spectrum of chalcone **S1-1** in $CDCl_3$

In-vitro assays

Cell viability assay

The cytotoxic activities of the newly synthesized chalcone derivatives **S1(1-2)** and **S2(1-2)** were evaluated for growth inhibitory activity against two breast cancer cell lines (MCF-7 and MDA-MB-231) and one non-cancerous cell line (MCF-10A). The assay utilized the well-established 3-[4,5-dimethylthiazol-2-yl]-2,5-diphenyltetrazolium bromide (MTT) assay with the use of tamoxifen as the positive control.

The cytotoxic activities of the tested compounds against cultured cell lines have been expressed as the IC_{50} values in μM while IC_{50} describes the concentration of the synthetic compound (inhibitor) which is required for 50% inhibition of the target *in-vitro*. The lower value of IC_{50} indicates stronger inhibition of cell proliferation. The IC_{50} values of the compounds against these human cancer cells are summarized in Table 2 and Figure 7. All the target compounds exhibited cytotoxicity activities with the IC_{50} values in the range of 2.04-100 μM.

Compounds **S1-1** and **S1-2** showed IC_{50} values of 2.23 and 2.04 μM, respectively, against MCF-7. These compounds exhibited IC_{50} values of 6.44 and 3.7 μM, respectively, against MDA-MB-231, which were found to possess higher cytotoxicity than the positive control, tamoxifen against both cell lines. MCF-7 is a breast cancer cell line associated with hormone receptors such as estrogen and progesterone (42). The hormonal breast cancer type is most likely found in non-metastatic cancer (43), which are relatively able to be stopped using common anti-breast cancer drugs such as tamoxifen. In contrast, the non-hormonal cancer type such as MDA-MB-231 was not too sensitive against tamoxifen due to its metastatic character (42). Therefore, according to the results, the most active compounds have selectively inhibited the non-metastatic cancer cell rather than the metastatic cancer cell. However, the results showed that the most active compounds, **S1-1** and **S1-2**, were slightly better than tamoxifen in inhibiting the non-metastatic cancer cell that could be a potential agent for breast anticancer.

Modification of compounds **S1-1** and **S1-2** core system of benzene-1,3,5-tri-chalcone with nitrilotri(benzene-1,3,5-tri-chalcone) of compounds **S2-1** and **S2-2** showed the IC_{50} values of 100 and 27.2 μM, respectively against MCF-7. For the other cell lines of MDA-MB-231 cell line, second series of the target compounds **S2(1-2)** exhibited moderate cytotoxicity activity (IC_{50} = 100 μM).

Molecular Docking and Molecular Dynamic simulations in the previous study (31) for chalcone **S1-1** and **S1-2** confirmed the strong cytotoxic activity over MCF-7. These two compounds showed the key interactions with EGFR kinase compared to others. The strong cytotoxicity effect of these compounds against cell proliferation screening is associated with their kinase inhibitory activities such as EGFR-TK phosphorylation (44-46). EGFR is found at high levels in cancer cells. The binding of chalcone compounds to EGFR causes autophosphorylation of the receptor tyrosine kinase. The inhibition EGFR-TK activity is the target for the most promising chemotherapeutic agent, leading to cancer cell death (47).

The degree of selectivity of the synthesized compounds was expressed as per previous reports with a minor modification. The higher the selectivity index (SI), the more promising a compound is. A value of SI below 2.0 indicates that while a compound possesses strong growth inhibitory activity, it may be a general toxin that is affecting normal cells equally (48). Based on this, the SI data shown in Table 2 indicates that compound **S1-1** and **S1-2** showed a high degree of cytotoxic selectivity against MCF-7, which exhibited an increased cytotoxic selectivity than the positive control, tamoxifen. On other hand, compounds **S2-1** and **S2-2** exhibited a lower degree of cytotoxic selectivity against MCF-7, showing an increased cytotoxicity toward the healthy cell.

Table 2: Cytotoxic effects of synthesized tri-chalcone derivatives against breast cancer cell lines (MCF-7, MDA-MB-231) and one non-cancerous cell lines (MCF-10A)

Compounds	IC_{50} (72 h) (μM)			Selectivity Index	
	MCF-7	MDA-MB-231	MCF-10A	MCF-7	MDA-MB-231
S1-1	2.23 ± 0.11	6.44 ± 0.01	12.73 ± 0.01	5.71	1.98
S1-2	2.04 ± 0.71	3.75 ± 0.26	12.59 ± 0.04	6.17	3.58
S2-1	100 ± 0.01	100 ± 0.01	100 ± 0.01	1	1
S2-2	27.2 ± 2.21	100 ± 0.01	4.86 ± 0.13	0.18	0.05
Tamoxifen	9.3 ± 0.44	18.92 ± 1.43	23.71 ± 0.99	2.54	1.25

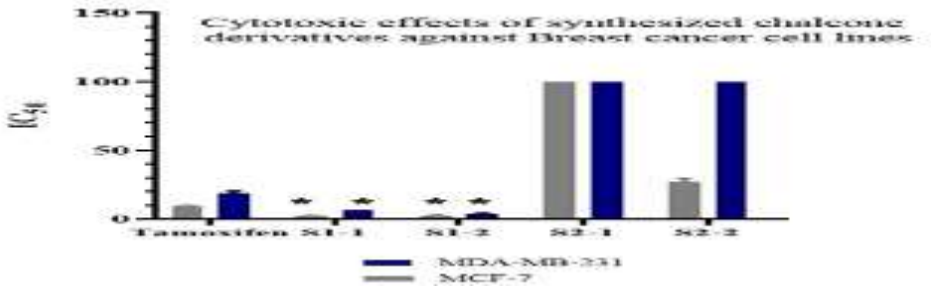

Figure 7: the cytotoxic activity of chalcone derivatives at 72 h in the inhibition of MCF-7 and MDA-MB-231 cells based on MTT assay. Data are expressed as mean±SEM of a representative experiment performed in triplicate (n = 3). * Symbol above the bars indicate significant differences. The significance was considered at P< 0.0001

Recombinant EGFR kinase assay

According to the MTT assay results, compound **S1-1** and **S1-2** were selected to study their ability to inhibit EGFR kinase specifically. The luminescence of ATP conversion was measured using ADP-Glo™ kinase assay at two different concentrations of 50 and 0.19 µM. Results indicated a significant inhibition of the recombinant kinase when incubated with the inhibitors. At the concentration of 50 µM, compound **S1-1** has managed to inhibit the enzyme with an 86% inhibition rate. On the other hand, compound **S1-2** showed an inhibition rate of 75% at the same concentration. However, when the concentration drops to 0.19 µM compound **S1-1** inhibition rate falls to 67% which is still considered as a significant inhibitory activity. Alternatively, compound **S1-2** has uncovered a superior inhibition rate of 83% at the concentration of 0.19 µM (Figure 8). This is consistent with the molecular docking results where compound **S1-2** has managed to achieve an extra conventional hydrogen bond that can strengthen its binding, although their binding affinity is relatively similar. Consequently, it also confirms the cytotoxicity and viability findings where compound **S1-2** showed a more potent cytotoxic activity compared to compound **S1-1**. This finding indicated the high potentials of these chalcone derivatives to be considered and additionally investigated for their anticancer activities.

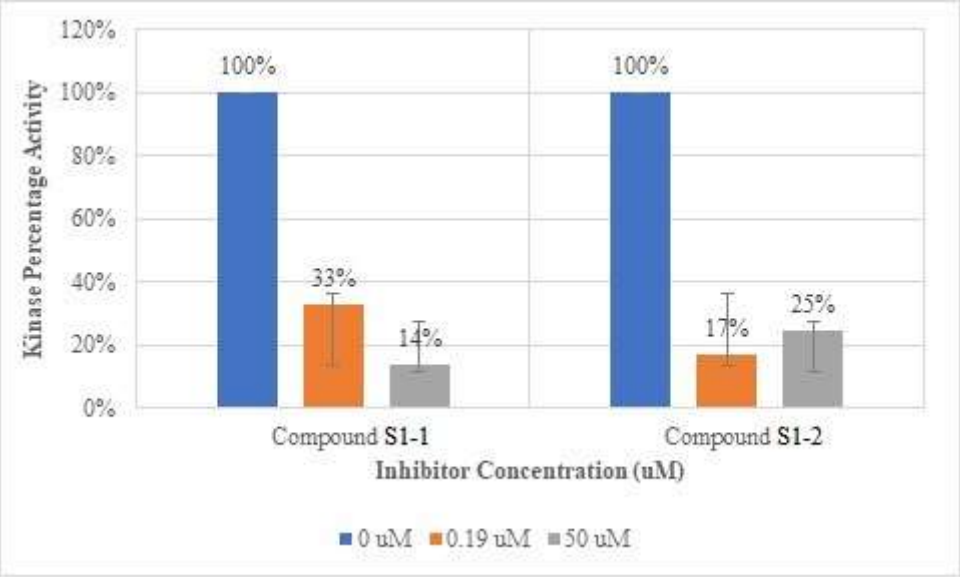

Figure 8: Recombinant kinase activity measured using ADP-Glo™ for compounds **S1-1** and **S1-2** at three different concentrations (0, 0.19 and 50 µM).

CONCLUSION

Fourteen chalcone derivatives with potential EGFR activity were studied and two compounds: **S1(1-2)** and **S2(1-2)** with promising EGFR inhibitory activity were synthesized and characterized. Molecular docking simulations showed that the tri-chalcone derivatives have sufficient EGFR binding affinity. The tri-chalcone derivatives (compound **S1-1** and **S1-2**) showed a high inhibitory potency through hydrogen bonding with LYS 745 and MET 793 (31) and this is crucial their EGFR inhibition and cytotoxicity activities. Compounds **S1-1** and **S1-2** showed a significant improvement in the anti-cancer resistant treatment due to their potential effects on the EGFR and the possible anti-ER effect. Compounds **S1-1** and **S1-2** showed the IC_{50} and SI values which indicated that these two compounds can be excellent candidates in treating hormonal breast, non-hormonal breast, and tamoxifen-resistant cases. Compounds **S1-1** and **S1-2** showed a potent cytotoxicity activity of MCF-7 (2.23 ± 0.11 and 2.04 ± 0.01 µM) and MDA-MB-231 (6.44 ± 0.11 and 3.75 ± 0.26 µM), respectively, relative to tamoxifen IC_{50} of 9.3 ± 0.44 and 18.92 ± 1.43 µM. Thus, *in-vitro* EGFR activity was evaluated and the specific kinase-inhibition activity for compounds **S1-1** and **S1-2** was found to be 67% and 83%, respectively, at a concentration as low as 0.19 µM. Thus, the findings showed that these compounds can be considered for advanced investigations in the development of potential anticancer agents.

Author contributions: Conceptualization, M.A., M.K. and B.O.A.; methodology, M.A., M.M.A., M.K., B.O.A., N.N.S.N.M.K. and M.M.; software, M.A., M.K. and B.O.A.; validation: M.A., B.O.A., N.N.S.N.M.K. and M.M.; investigation, M.A., M.K. and B.O.A.; writing-original draft, M.A. and M.K.; writing-review and editing, M.K., B.O.A., and M.H.; supervision, M.K. and B.O.A.

ACKNOWLEDGEMENT

This work was financially supported by the Fundamental Research Grant Scheme (FRGS) 1/2019 (203.PKIMIA.6711789). The author wants to thank the Kementerian Pengajian Tinggi (KPT), Malaysia and Universiti Sains Malaysia.

Conflicts of Interest: The authors declare no conflict of interest related to this work.

REFERENCES

1. Perazella MA. Onco-nephrology: renal toxicities of chemotherapeutic agents. Clinical Journal of the American Society of Nephrology. 2012;7(10):1713-21.
2. Dasari S, Tchounwou PB. Cisplatin in cancer therapy: molecular mechanisms of action. European journal of pharmacology. 2014;740:364-78.

3. Thavendiranathan P, Wintersperger BJ, Flamm SD, Marwick TH. Cardiac MRI in the assessment of cardiac injury and toxicity from cancer chemotherapy: a systematic review. Circulation: Cardiovascular Imaging. 2013;6(6):1080-91.
4. Zhang L, Yu Q, Wu X-C, Hsieh M-C, Loch M, Chen VW, *et al*. Impact of chemotherapy relative dose intensity on cause-specific and overall survival for stage I–III breast cancer: ER+/PR+, HER2-vs. triple-negative. Breast cancer research and treatment. 2018;169(1):175-87.
5. Sommariva S, Pongiglione B, Tarricone R. Impact of chemotherapy-induced nausea and vomiting on health-related quality of life and resource utilization: a systematic review. Critical reviews in oncology/hematology. 2016;99:13-36.
6. Sibaud V, Lebœuf NR, Roche H, Belum VR, Gladieff L, Deslandres M, *et al*. Dermatological adverse events with taxane chemotherapy. European Journal of Dermatology. 2016;26(5):427-43.
7. Tang Y, Soroush F, Tong Z, Kiani MF, Wang B. Targeted multidrug delivery system to overcome chemoresistance in breast cancer. International journal of nanomedicine. 2017;12:671.
8. Ji X, Lu Y, Tian H, Meng X, Wei M, Cho WC. Chemoresistance mechanisms of breast cancer and their countermeasures. Biomedicine & Pharmacotherapy. 2019;114:108800.
9. Huang L, Fu L. Mechanisms of resistance to EGFR tyrosine kinase inhibitors. Acta Pharmaceutica Sinica B. 2015;5(5):390-401.
10. Massarweh S, Osborne CK, Creighton CJ, Qin L, Tsimelzon A, Huang S, *et al*. Tamoxifen resistance in breast tumors is driven by growth factor receptor signaling with repression of classic estrogen receptor genomic function. Cancer research. 2008;68(3):826-33.
11. Li G, Zhang J, Jin K, He K, Zheng Y, Xu X, *et al*. Estrogen receptor-α36 is involved in development of acquired tamoxifen resistance via regulating the growth status switch in breast cancer cells. Molecular oncology. 2013;7(3):611-24.
12. Sharma N, Sharma M, Jamal QMS, Kamal MA, Akhtar S. Nanoinformatics and biomolecular nanomodeling: a novel move en route for effective cancer treatment. Environmental Science and Pollution Research. 2019:1-15.
13. Gee JMW, Harper M, Hutcheson I, Madden T, Barrow D, Knowlden J, *et al*. The antiepidermal growth factor receptor agent gefitinib (ZD1839/Iressa) improves antihormone response and prevents development of resistance in breast cancer in vitro. Endocrinology. 2003;144(11):5105-17.
14. Mok TS, Lee K, Leung L, editors. Targeting epidermal growth factor receptor in the management of lung cancer. Seminars in oncology; 2014: Elsevier.
15. Chen Y-M. Update of epidermal growth factor receptor-tyrosine kinase inhibitors in non-small-cell lung cancer. Journal of the Chinese medical Association. 2013;76(5):249-57.
16. Goffin JR, Zbuk K. Epidermal growth factor receptor: pathway, therapies, and pipeline. Clinical therapeutics. 2013;35(9):1282-303.
17. Elkhalifa D, Alali F, Al Moustafa A-E, Khalil A. Targeting triple negative breast cancer heterogeneity with chalcones: a molecular insight. Journal of drug targeting. 2019;27(8):830-8.
18. Qin HL, Leng J, Youssif BG, Amjad MW, Raja MAG, Hussain MA, *et al*. Synthesis and mechanistic studies of curcumin analog-based oximes as potential anticancer agents. Chemical biology & drug design. 2017;90(3):443-9.
19. Starok M, Preira P, Vayssade M, Haupt K, Salomé L, Rossi C. EGFR inhibition by curcumin in cancer cells: a dual mode of action. Biomacromolecules. 2015;16(5):1634-42.
20. Wada K, Lee J-Y, Hung H-Y, Shi Q, Lin L, Zhao Y, *et al*. Novel curcumin analogs to overcome EGFR–TKI lung adenocarcinoma drug resistance and reduce EGFR–TKI-induced GI adverse effects. Bioorganic & medicinal chemistry. 2015;23(7):1507-14.
21. Lee J-Y, Lee Y-M, Chang G-C, Yu S-L, Hsieh W-Y, Chen JJ, *et al*. Curcumin induces EGFR degradation in lung adenocarcinoma and modulates p38 activation in intestine: the versatile adjuvant for gefitinib therapy. PloS one. 2011;6(8):e23756.
22. Xu Y-Y, Cao Y, Ma H, Li H-Q, Ao G-Z. Design, synthesis and molecular docking of α, β-unsaturated cyclohexanone analogous of curcumin as potent EGFR inhibitors with antiproliferative activity. Bioorganic & medicinal chemistry. 2013;21(2):388-94.
23. Bayomi SM, El-Kashef HA, El-Ashmawy MB, Nasr MN, El-Sherbeny MA, Badria FA, *et al*. Synthesis and biological evaluation of new curcumin derivatives as antioxidant and antitumor agents. Medicinal Chemistry Research. 2013;22(3):1147-62.
24. Youssef KM, El-Sherbeny MA, El-Shafie FS, Farag HA, Al-Deeb OA, Awadalla SAA. Synthesis of curcumin analogues as potential antioxidant, cancer chemopreventive agents. Archiv der Pharmazie: An International Journal Pharmaceutical and Medicinal Chemistry. 2004;337(1):42-54.
25. Manojkumar P, Ravi T, Subbuchettiar G. Synthesis of coumarin heterocyclic derivatives with antioxidant activity and in vitro cytotoxic activity against tumour cells. Acta Pharmaceutica. 2009;59(2):159-70.
26. Bayomi SM, El-Kashef HA, El-Ashmawy MB, Nasr MN, El-Sherbeny MA, Abdel-Aziz NI, *et al*. Synthesis and biological evaluation of new curcumin analogues as antioxidant and antitumor agents: molecular modeling study. European journal of medicinal chemistry. 2015;101:584-94.
27. Yang EB, Guo YJ, Zhang K, Chen YZ, Mack P. Inhibition of epidermal growth factor receptor tyrosine kinase by chalcone derivatives. Biochimica et Biophysica Acta (BBA)-Protein Structure and Molecular Enzymology. 2001;1550(2):144-52.
28. Rao GE, Rahaman SA, Rani AP. Insights from molecular modeling, docking and simulation of imidazole nucleus containing chalcones with EGFR kinase domain for improved binding function. Bioinformation. 2016;12(2):48.
29. Shin SY, Yoon H, Ahn S, Kim D-W, Kim SH, Koh D, *et al*. Chromenylchalcones showing cytotoxicity on human colon cancer cell lines and in silico docking with aurora kinases. Bioorganic & medicinal chemistry. 2013;21(14):4250-8.
30. Elias D, Beazely M, Kandepu N. Bioactivities of chalcones. Curr Med Chem. 1999;6(12):1125-49.
31. Al-Anazi M, Al-Najjar B, Khairuddean M. Structure-Based Drug Design Studies Toward the Discovery of Novel Chalcone Derivatives as Potential Epidermal Growth Factor Receptor (EGFR) Inhibitors. Molecules. 2018;23(12):3203.

32. Aertgeerts K, Skene R, Yano J, Sang BC, Zou H, Snell G, *et al*. Structural analysis of the mechanism of inhibition and allosteric activation of the kinase domain of HER2 protein. Journal of Biological Chemistry. 2011;286(21):18756-65.
33. Morris GM, Goodsell DS, Halliday RS, Huey R, Hart WE, Belew RK, *et al*. Automated docking using a Lamarckian genetic algorithm and an empirical binding free energy function. Journal of computational chemistry. 1998;19(14):1639-62.
34. Morris GM, Huey R, Lindstrom W, Sanner MF, Belew RK, Goodsell DS, *et al*. AutoDock4 and AutoDockTools4: Automated docking with selective receptor flexibility. Journal of computational chemistry. 2009;30(16):2785-91.
35. Claisen L, Claparède A. Condensationen von ketonen mit aldehyden. Berichte der deutschen chemischen Gesellschaft. 1881;14(2):2460-8.
36. Schmidt JG. Ueber die Einwirkung von Aceton auf Furfurol und auf Bittermandelöl bei Gegenwart von Alkalilauge. Berichte der deutschen chemischen Gesellschaft. 1881;14(1):1459-61.
37. Kollman PA, Massova I, Reyes C, Kuhn B, Huo S, Chong L, *et al*. Calculating structures and free energies of complex molecules: combining molecular mechanics and continuum models. Accounts of chemical research. 2000;33(12):889-97.
38. Pao W, Miller V, Zakowski M, Doherty J, Politi K, Sarkaria I, *et al*. EGF receptor gene mutations are common in lung cancers from "never smokers" and are associated with sensitivity of tumors to gefitinib and erlotinib. Proceedings of the National Academy of Sciences. 2004;101(36):13306-11.
39. Barker A. Genistein analogues: effects on epidermal growth factor receptor tyrosine kinase and on stress-activated pathways. Bioorg Med Chem. 2001;11:1911-4.
40. Mahajan P, Suri N, Mehra R, Gupta M, Kumar A, Singh SK, *et al*. Discovery of novel small molecule EGFR inhibitory leads by structure and ligand-based virtual screening. Medicinal Chemistry Research. 2017;26(1):74-92.
41. Subrahmanyam RS, Ramesh PK, B.S., Swaroop S, Khan MA, Darla MM, K A, *et al*. SYNTHESIS AND BIOLOGICAL EVALUATION OF SOME NEW CLASS OF CHROMENOIMIDAZOLE DERIVATIVES AS PROBABLE ANTI CANCER AGENTS. Rasayan journal of chemistry. 2017;10(4):1194-212.
42. Holliday DL, Speirs V. Choosing the right cell line for breast cancer research. Breast cancer research. 2011;13(4):215.
43. Roviello G, Michelet MG, D'Angelo A, Nobili S, Mini E. Role of novel hormonal therapies in the management of non-metastatic castration-resistant prostate cancer: a literature-based meta-analysis of randomized trials. Clinical and Translationsssal Oncology. 2019:1-7.
44. Wang H-C, Yan X-Q, Yan T-L, Li H-X, Wang Z-C, Zhu H-L. Design, synthesis and biological evaluation of benzohydrazide derivatives containing dihydropyrazoles as potential EGFR kinase inhibitors. Molecules. 2016;21(8):1012.
45. Mohameda AA, Badriab FA, Maaroufa AR, Abdel-Aziza NI, ElSendunyc F, Abdel-Aziza AA, *et al*. Synthesis, antitumor evaluation and molecular modeling study of novel benzimidazoles and pyrazinobenzimidazoles. Journal of Applied Pharmaceutical Science. 2017;7(06):206-14.
46. Mphahlele M, Maluleka M, Parbhoo N, Malindisa S. Synthesis, evaluation for cytotoxicity and molecular docking studies of benzo [c] furan-chalcones for potential to inhibit tubulin polymerization and/or EGFR-tyrosine kinase phosphorylation. International journal of molecular sciences. 2018;19(9):2552.
47. Arteaga CL. Epidermal growth factor receptor dependence in human tumors: more than just expression? The oncologist. 2002;7(Supplement 4):31-9.
48. Badisa RB, Darling-Reed SF, Joseph P, Cooperwood JS, Latinwo LM, Goodman CB. Selective cytotoxic activities of two novel synthetic drugs on human breast carcinoma MCF-7 cells. Anticancer research. 2009;29(8):2993-6.